27th International Pittsburgh Coal Conference
October 11–14, 2010, Istanbul, Turkey

FORCED FLAME RESPONSE MEASUREMENT IN A GAS TURBINE COMBUSTOR WITH HIGH HYDROGEN FUEL

K.T. Kim*, J.G. Lee, B.D. Quay, D.A. Santavicca
Center for Advanced Power Generation
Department of Mechanical and Nuclear Engineering
The Pennsylvania State University, University Park, PA, 16802

ABSTRACT

The forced response of swirl-stabilized lean-premixed turbulent flames to acoustic oscillations in a hydrogen enriched laboratory-scale gas turbine combustor was experimentally investigated. Nonlinear flame transfer function measurements were taken to investigate the flame's heat release response to upstream acoustic perturbations. This analysis shows that the dynamics of natural gas-air premixed flames are characterized by several regimes: the linear, transition, and first and second nonlinear regimes, depending upon steady-state flame geometry, modulation frequency, and amplitude of excitation. The present results show that the flame geometry changes from a dihedral V flame to an enveloped M flame with an increase in hydrogen mole fraction, and the changes in steady-state flame structures have a significant impact on the flame's response to acoustic modulations. The present results suggest that the M flame, unlike the V flame, has the unique dynamic characteristic of acting as a damper of flow perturbations. The response of the M flame remains in the linear regime, irrespective of the shedding of a vortex-ring structure, because the interaction between the large-scale structure and the flame is not strongly coupled.

INTRODUCTION

Combustion instabilities are characterized by large-amplitude pressure oscillations that are driven by unsteady heat release. It is by nature a self-excited oscillation, involving complicated physical phenomena such as unsteady combustion, acoustic fluctuations, heat transfer, and the vorticity field. These high-amplitude pressure oscillations can substantially reduce the performance of a system and in extreme cases can cause structural damage to engines. Over the last two decades, a large number of studies using experimental [1-4], theoretical [5-8], and CFD simulation [9-11] approaches have been performed to investigate instability mechanisms, controlling parameters, and active or passive control methodologies to suppress the instability intensity level to acceptable ranges. Recently, Huang and Yang [12] have provided comprehensive reviews on this issue. Ultimately, to accurately predict instability characteristics at the development stage, a complete understanding of the nature of combustion instabilities will be required and sophisticated theoretical models must be developed to incorporate the complex flame dynamics into the prediction model.

Development of a theoretical model capable of predicting the formation of thermoacoustic pulsations is contingent on a physical understanding of the linear and nonlinear responses of a flame to periodic disturbances. When there are no equivalence ratio oscillations in the mixing plenum, the response of a premixed flame is primarily governed by acoustic velocity fluctuations. To quantitatively describe the response of a flame to acoustic forcing, the nonlinear flame transfer function (FTF) is introduced, defined as the normalized ratio of heat release and velocity fluctuations:

$$FTF(f,A)=\frac{Q'(f)/\overline{Q}}{V'(f)/\overline{V}} \quad (1)$$

where $\overline{Q}$ is the time-averaged heat release rate, $\overline{V}$ is the mean velocity of the mixture in the mixing section, $Q'(f)$ and $V'(f)$ are their corresponding amplitudes at the forcing frequency, f, and A is the magnitude of $V'(f)/\overline{V}$. The flame transfer function can be obtained by experimental [2-4, 13-14], theoretical [6-8], or numerical [5] methods. The flame transfer function provides an insight into the response of a flame to inlet disturbances, and it can be mathematically formulated and used in the thermoacoustic network modeling as a source term to predict self-induced combustion instability [14].

In the present article, the effects of fuel composition on the forced response of a swirled lean-premixed flame are experimentally investigated. Development of fuel-flexible gas turbine engines capable of operating with highly variable and potentially low quality fuels, such as coal-derived syngas fuels, while producing minimal air pollutants, is a key issue in the gas turbine combustion community [15-16]. Most previous studies on the effects of fuel composition on applications in gas turbines have dealt with static stabilities, pollutant emissions [17-20], flame propagation speed [21-23], and steady-state flame structures [24-25]. It was found that the addition of hydrogen to hydrocarbon fuels results in a significant increase in OH radical concentration, extending the lean stability limits and increasing flame propagation speeds. However, there have been relatively few experimental investigations on the influence

* Corresponding author: University of Cambridge, Engineering Department, Trumpington Street, Cambridge, CB2 1PZ, UK. E-mail address: ktk23@cam.ac.uk.

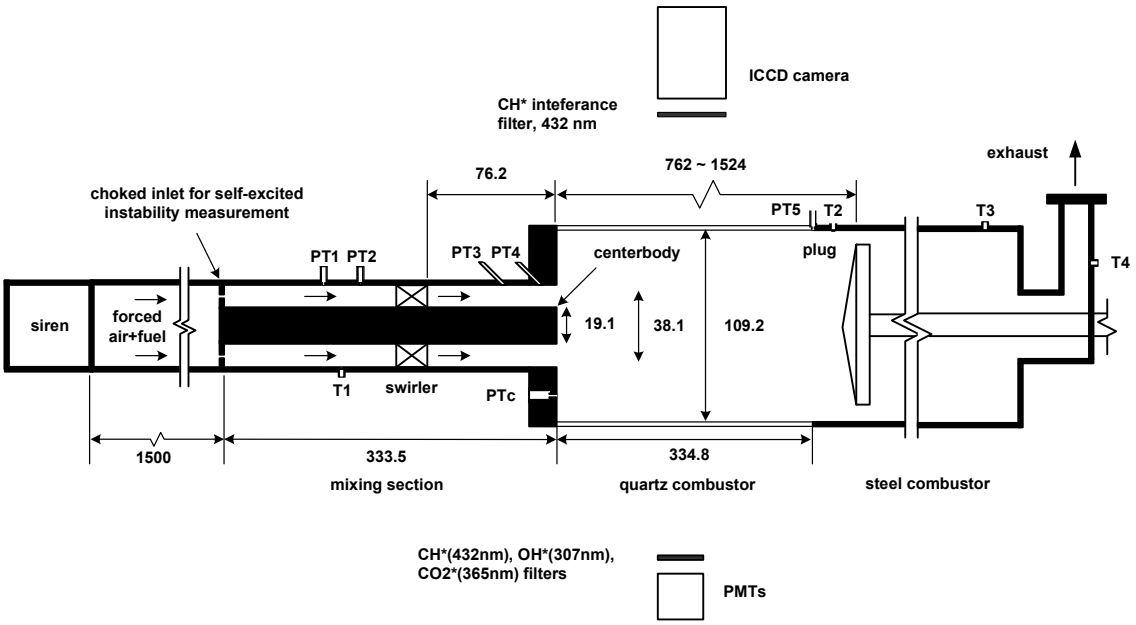

Figure 1. Schematic of a swirl-stabilized, lean-premixed, model gas turbine combustor. Dimensions in millimeters.

of fuel composition (particularly, hydrogen-enrichment) on combustion dynamics [26-27]. It is not possible to make general statements about the impact of fuel composition variation upon a combustor's propensity to become unstable– the effects can be either stabilizing or destabilizing.

In the present paper, we focus on the linear/nonlinear dynamics of H_2-enriched, swirl-stabilized, lean-premixed flames using a phase-resolved analysis and nonlinear flame transfer function measurements. Two key mechanisms of nonlinearity, i.e., shear layer rollup and unsteady flame liftoff for dihedral V flames, are examined. In particular, the dynamics of H_2-enriched enveloped M-shaped flames are compared with pure natural gas flames with inverted dihedral V flame geometry. It is shown that modification of steady-state flame structures significantly affects the linear and nonlinear dynamics of a laminar premixed flame [28]. The present results suggest that the M flames do not exhibit the strong overshoot behavior which is observed in the case of dihedral V flames. This study extends previous experimental and analytical results from laminar to turbulent premixed flames.

EXPERIMENTAL METHODS

Lean Premixed Gas Turbine Combustor

A schematic of the experimental setup is shown in Figure 1. This facility consists of an air inlet section, a siren, a mixing section, an optically-accessible quartz combustor section, a steel combustor section, and an exhaust section. The air can be heated to a maximum temperature of 400 °C by a 30 kW electric heater. A siren-type modulation device (rotor + stator) is used to provide acoustic modulations. The siren is driven by a variable-speed DC motor, providing capabilities for changing forcing frequency (~ 500 Hz). Two high-temperature globe valves are used to control the bypass flow rate, i.e., the inlet velocity fluctuation amplitudes. The mixing section is 0.333 m long and has an annular cross-section that is defined by a 19.1 mm O.D. centerbody and a 38.1 mm I.D. mixing tube. The centerbody is centered in the mixing tube, and it is positioned such that its downstream end is flush with the combustor dump plane. A 30^o flat-vane axial swirler is mounted in the mixing tube 76.2 mm upstream of the combustor dump plane. At the entrance to the mixing section the flow is choked. This provides a well-defined acoustic boundary condition for self-excited instability measurements. For forced flame response measurements, the choking plate is removed and mounted upstream of the siren. Fuel (natural gas + H_2) is injected and mixed upstream of the choked inlet in order to ensure that the reactant mixtures are spatially and temporally homogeneous before they enter the reaction zone.

The combustor consists of a stainless steel dump plane, to which an optically accessible fused-silica combustor with a diameter of 109.2 mm and length of 334.8 mm is attached. The downstream end of the quartz combustor is connected to a stainless steel variable-length combustor section. The length of the combustor can be continuously varied between 762 mm and 1524 mm by moving a water-cooled plug along the length of the steel combustor section. For forced response measurements, the combustor length was maintained at the minimum to minimize the influence of system acoustics on upstream acoustic excitation.

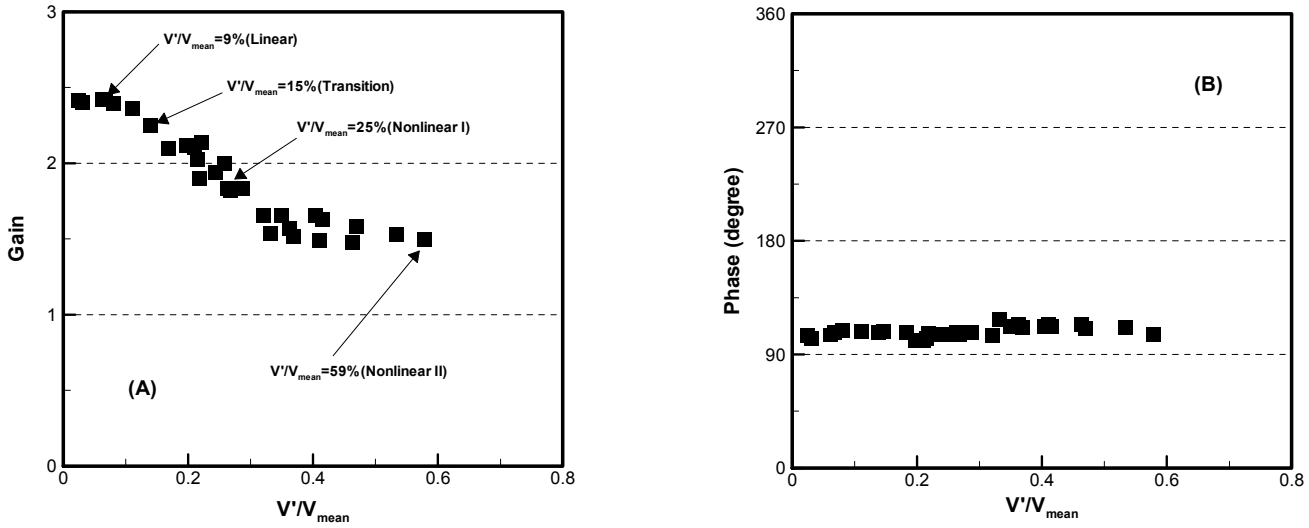

Figure 2. (A) The gain and (B) phase of flame transfer function as a function of the magnitude of inlet velocity perturbation at a modulation frequency of 200 Hz. Inlet conditions: T_{in} = 200 °C, V_{mean} = 60 m/s, ϕ = 0.60, and X_{H2} = 0.00.

Instrumentation and Test Conditions

High frequency-response, water-cooled, piezoelectric pressure transducers (PCB 112A04) were used to measure pressure perturbations in the mixing (denoted by PT1−PT4 in Figure 1) and the combustor sections (PTc and PT5). The pressure signals were conditioned by amplifiers, digitized by an analog-to-digital converter, and stored in microcomputer memory for processing at a sampling rate of 8192 Hz. A total of 16,384 data points were taken during each test, resulting in a frequency resolution of 0.5 Hz and a time resolution of 0.122 msec. Spectral analysis of the signals was performed using the fast Fourier transform (FFT) technique. Two pressure transducers located at 12.7 mm (PT4) and 50.8 mm (PT3) upstream of the combustor dump plane were used to estimate the inlet velocity fluctuations using the two-microphone method. To calibrate the two-microphone method, direct measurements of velocity fluctuations were performed under cold flow conditions with a hot wire anemometer (TSI 1210-20). A photomultiplier tube (PMT, Hamamatsu model H7732-10) was used to measure the global CH* (432 ± 5 nm) chemiluminescence emission intensities from a whole flame. An ICCD camera (Princeton Instruments model 576G) with a CH* band pass filter centered at 430 nm (10 nm FWHM) was used to record the flame images. For phase-averaged imaging, the ICCD camera was synchronized with the combustor pressure signal and fifty averaged images were taken over a cycle of oscillation with a phase interval of 30°. The phase angle φ = 0° corresponds to the positive-to-negative zero transition, and φ = 270° to the maximum combustor pressure. Because CH* chemiluminescence images are line-of-sight integrated images, a three-point Abel deconvolution scheme was used to extract two-dimensional information from the line-of-sight images.

All tests were performed at a mean pressure of 1 atm and at mean equivalence ratio of 0.60. Mean velocity at the nozzle was 60 m/s and the inlet temperature was kept constant at 200 °C, giving a Reynolds number of approximately 33,000. Forcing frequencies were varied from 100 to 400 Hz (Δf = 25 Hz). The frequency range of 100−400 Hz includes two distinct frequencies at limit cycle oscillations observed in the lean premixed gas turbine combustor [27]. H_2-blended (based on volume) natural gas fuels with X_{H2} = 0.00 and 0.30 were used to examine the impacts of fuel composition variation upon the response of the flame to acoustic excitation.

RESULTS AND DISCUSSION

Linear and Nonlinear Dynamics of Inverted Dihedral V Flames

Experiments were performed wherein the heat release response of hydrogen-enriched natural gas-air premixed flames to acoustic forcing was determined for various levels of inlet velocity oscillations. Under the conditions investigated here, the highest perturbation levels are not determined by flame blowoff, but by limitation of the modulating device. The magnitude of upstream forcing which can be achieved by the device is contingent on modulation frequency. It was observed that the maximum amplitude can be attained at a modulation frequency of near 200 Hz, inasmuch as the combustor mixing section with upstream plenum acts as a resonator with peak responses around that frequency. The frequency, $f \approx$ 200 Hz, also corresponds to one of the self-excited instability frequencies observed in the test rig [27]. In the present study, the flame

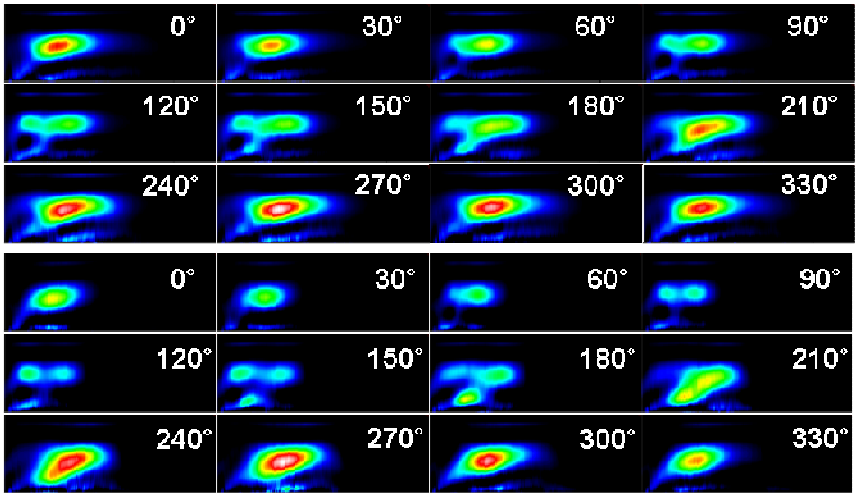

Figure 3. Phase-synchronized deconvoluted CH* chemiluminescence images at a modulation frequency of 200 Hz for (A) V'/V_{mean} = 9%(top) and (B) V'/V_{mean} = 15%(bottom). The intensity is displayed in linear pseudo color scale that white denotes the highest intensity and black means the lowest intensity. Inlet conditions: T_{in} = 200 °C, V_{mean} = 60 m/s, ϕ = 0.60, and X_{H2} = 0.00.

transfer function measurements were performed at a modulation frequency of 200 Hz for different fuel compositions. It is believed that the response of the flame at f = 200 Hz will help to illuminate the flame dynamics under limit-cycle oscillations at a frequency near 200 Hz.

Figure 2 presents the amplitude dependence of the gain and phase of the flame transfer function (see Eq. 1) at a modulation frequency of 200 Hz. These measurements were made at an inlet temperature of 200 °C, mean nozzle velocity of 60 m/s, mean equivalence ratio of 0.60, and hydrogen mole fraction of 0.00. The global CH* chemiluminescence intensities were used as an indicator of heat release rate oscillations, based on experimental observation that CH* chemiluminescence intensity increases linearly with fuel flow rate at a given overall equivalence ratio. The coherence function between inlet velocity and CH* chemiluminescence intensity was measured to close to unity at the forcing frequency of 200 Hz, enabling flame transfer functions to be accurately determined. Also, a high velocity perturbation magnitude of up to approximately 60% can be achieved at this forcing frequency. At these inlet conditions, the flame is stabilized in the inner shear layer and it is attached to the centerbody, exhibiting an inverted dihedral V structure [14].

The responses of the dihedral V flame to acoustic perturbations are divided into several regimes, as shown in Figure 2. In the linear regime (V'/V_{mean} < 10%), the normalized heat release response increases linearly with the amplitude of excitation; thus, the gain is almost constant. When the magnitude of inlet velocity fluctuation is greater than 10%, the gain decreases with an increase in perturbation amplitude, representing typical nonlinear behavior. It is noteworthy that when the modulation amplitude is greater than 40% of the mean value, the normalized CH* chemiluminescence intensity levels off again. Similar characteristics of acoustically forced swirl-stabilized flames were also observed by Thumuluru and Lieuwen [29]. They state that the flame's heat release response exhibits multiple saturating behaviors and a non-monotonic dependence upon amplitude. Phase-resolved flame imaging measurements in each regime will elucidate the amplitude-dependent dynamic characteristics of acoustically forced swirl flames. Figure 2 (B) shows that the phase measured between the CH* chemiluminescence signal and the inlet velocity fluctuation is essentially independent of the modulation amplitude up to V'/V_{mean} = 0.60. This is consistent with previous studies on laminar premixed flames [28], and indicates that the frequency-dependent convection times for a velocity perturbation to reach the flame are not a function of the modulation amplitude, irrespective of linear and nonlinear regimes.

To identify the key physical processes associated with the linear/nonlinear response of the dihedral V flame to flow forcing, phase-averaged chemiluminescence emission from the whole flame was recorded using an intensified CCD camera. Figure 3 presents a sequence of phase-synchronized CH* chemiluminescence images at a modulation frequency of 200 Hz during a period of oscillation for excitation amplitudes of (A) V'/V_{mean} = 9% and (B) 15%. They represent the response of the flame in the linear and transition regimes, respectively. Note that only the upper half of these deconvoluted images is shown, because the reconstructed images are axisymmetric. The direction of flow is from left to right. It can be observed from Figure 3 (A) that the flame moves back and forth due to the velocity oscillation in the annular jet region, and the reaction zone is located in the inner shear layer. Reaction occurs in the corner recirculation zone (CRZ) at φ = 90 ~ 180° when the

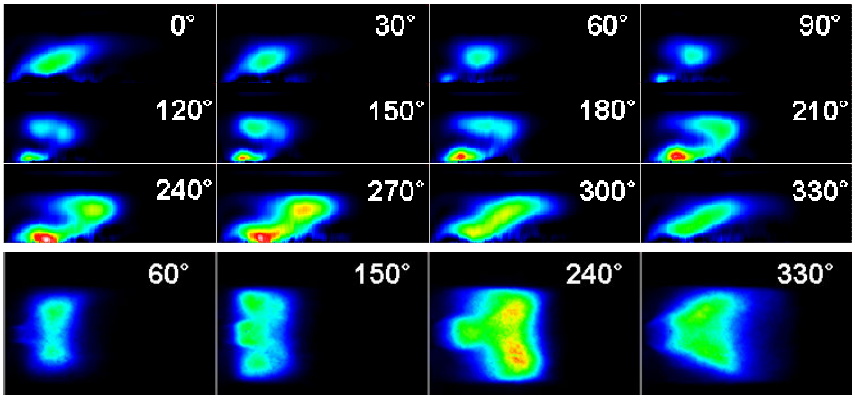

Figure 4. (A) Phase-synchronized deconvoluted CH* chemiluminescence images at modulation frequency of 200 Hz and V'/V_{mean} = 25% (top). (B) Line-of-sight integrated, background-corrected CH* chemiluminescence images at φ = 60, 150, 240, and 330° (bottom). Inlet conditions: T_{in} = 200 °C, V_{mean} = 60 m/s, ϕ = 0.60, and X_{H2} = 0.00.

flame moves upstream. Evolution of flame surface area by shear layer rollup is not seen because the minimum excitation level for the formation of a large-scale coherent structure is not achieved. Figure 3 (B) shows the forced flame response in the transition regime. The flame shapes at each phase are similar to those of the linear flame behavior, displayed in Figure 3 (A). The formation and reaction of large-scale, coherent vortex structures are, however, observed at φ = 180 ~ 270°. They are convected by the mean flow, and the heat release reaches its maximum at φ = 270°. The vortices periodically entrain a large amount of combustible material into the reaction zone at the modulation frequency, and therefore the temporal variations of flame surface area are determined by the interplay between the coherent structure and the flame.

Deconvoluted and line-of-sight integrated phase-averaged CH* chemiluminescence images in the first nonlinear regime are shown in Figures 4 (A) and (B), respectively. All inlet conditions are the same as for Figure 3, except for the modulation amplitude. The most distinct difference in flame behavior between the transition and the first nonlinear regimes is that in the first nonlinear regime, the flame front bends toward the inner recirculation zone at φ = 270°, as compared to the deconvoluted flame image at φ = 270° in Figure 3 (B). The interaction between a vortex-ring structure and the flame is significant at φ = 180° ~ 300°. The line-of-sight integrated images at φ = 150° and φ = 240° clearly show the vortex rollup and convection processes, respectively. It has been reported that the nonlinear response of premixed flames is related to the shear layer rollup [2, 4, 14, 29]. The shear layer rollup shortens the flame length, which in turn decreases the flame area in a nonlinear manner. Hence, the gain of the flame transfer function decreases in the nonlinear regime, as shown in Figure 2.

Figure 5 shows phase-resolved flame images at a modulation amplitude of 59%, corresponding to the second nonlinear regime. Note that the normalized CH* chemiluminescence intensity is constant with respect to the amplitude of excitation when V'/V_{mean} is greater than 40%. It is expected that the nonlinear dynamics of the flame is influenced by different controlling physics than in the first nonlinear response regime. The deconvoluted and line-of-sight integrated images at φ = 330° clearly show the unsteady flame liftoff from the attachment point. The high level of inlet velocity perturbation causes the flame attachment point to move off of the centerbody to the downstream inner recirculation zone. This indicates that when the inlet velocity perturbation magnitude is greater than 40% of the mean value, the dynamics of swirl-stabilized premixed flames subjected to upstream acoustic forcing are less influenced by the flame-vortex interaction. The unsteady flame liftoff (flame holding) plays a dominant role in the flame dynamics, due to the high perturbation amplitude. At V'/V_{mean} > 40%, a vortex ring structure is shed (see φ = 150° in Figure 5), and it is convected with the mean flow in the annular jet region, but the main reaction region is located in the inner recirculation zone. Therefore, the response levels off when the magnitude of acoustic forcing is greater than 40%, as shown in Figure 2.

To quantitatively describe the spatial distribution of the flame's heat release depending on excitation amplitudes, coordinates of maximum CH* chemiluminescence intensity locations at φ = 270° for perturbation levels of V'/V_{mean} = 9, 15, 25, and 59% are plotted in Figure 6. It clearly shows that with increasing modulation amplitude, the intense reaction region moves toward the inner recirculation zone. In consequence, the key mechanism of nonlinearity is modified from shear layer rollup to unsteady flame liftoff, depending on perturbation amplitude. The amplitude-dependent dynamics of inverted V flames suggest that limit-cycle pressure oscillation magnitudes are also governed by different mechanisms of flame area modulation under self-sustained oscillations, depending on the magnitude of inlet velocity fluctuation. An experimental investigation of the dynamics of self excited flames and a

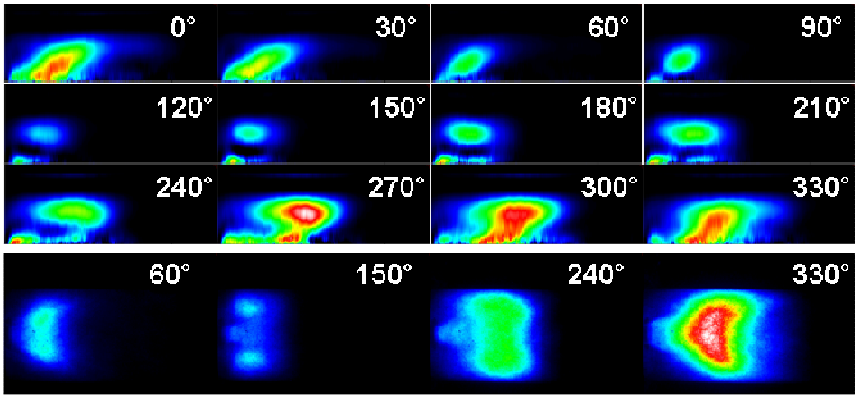

Figure 5. (A) Phase-synchronized deconvoluted CH* chemiluminescence images at modulation frequency of 200 Hz and V'/V_{mean} = 59% (top). (B) Line-of-sight integrated, background-corrected CH* chemiluminescence images at φ = 60, 150, 240, and 330° (bottom). Inlet conditions: T_{in} = 200 °C, V_{mean} = 60 m/s, ϕ = 0.60, and X_{H2} = 0.00.

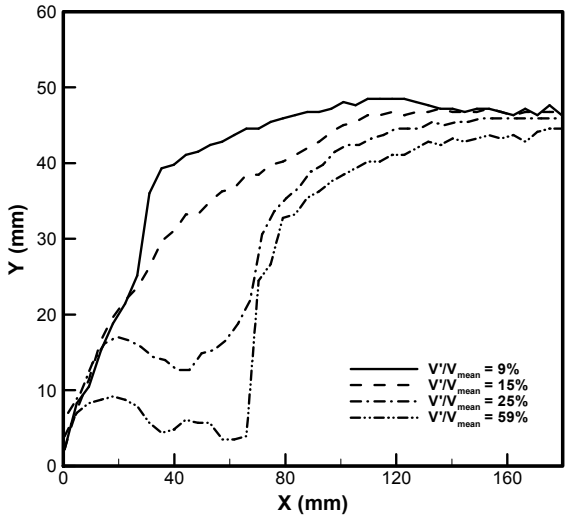

Figure 6. Coordinates of maximum CH* chemiluminescence intensity location at phase of φ = 270° (maximum CH* intensity) for inlet velocity magnitudes of V'/V_{mean} = 9, 15, 25, and 59%.

comparison between acoustically forced flames and flames under limit cycle oscillations are left for future studies.

Forced Response of H_2-Enriched Enveloped M Flames

In previous work [27], the authors have provided details on the modification of stable flame configurations, depending upon H_2 volume fraction in composite fuels. It has been shown that the flame geometry changes from an inverted dihedral V structure to an enveloped M geometry with increasing H_2 mole fraction. The M flames have unique characteristics that allow them to damp flow perturbations, as compared to V flames. Thus, the flame transfer function gain of enveloped M flames is much smaller than that of V flames for a given forcing frequency and amplitude. This is qualitatively consistent with theoretical and experimental studies on the response of laminar premixed flames by Schuller et al. [28, 30-31]. They described V flame behavior as an amplifier of flow perturbation in a certain range of frequencies, with the gain of laminar V flames being greater than that of conical and M-shaped flames. In this section, we will discuss the manner in which the combustion instability characteristics of a given gas turbine combustor are impacted by hydrogen levels in the fuel.

The amplitude dependence of the normalized CH* chemiluminescence emission intensity at a modulation frequency of 200 Hz for a H_2-enriched M flame with an enveloped geometry is shown in Figure 7. All inlet conditions are the same as for Figure 2, except for H_2 mole fraction. Hydrogen blended natural gas fuel (30% H_2 + 70% natural gas) was used and the overall equivalence ratio was kept constant at $\phi_{overall}$ = 0.60. It can be observed from Figure 7 that the normalized CH* chemiluminescence intensity increases linearly with the amplitude of excitation up to approximately V'/V_{mean} = 50%, indicating that the flame behaves linearly with respect to flow perturbations. The fact that the response of the flame remains in the linear regime even at a high perturbation amplitude of 50% is an unexpected result. As previously shown in Figures 4 and 5, excitation of a large scale coherent structure plays an important role in inducing nonlinearity when the normalized acoustic velocity amplitude is greater than 25% at a frequency of 200 Hz. Considering that the formation and convection of the structure are governed by fluid dynamic conditions, not by fuel composition, it can be supposed that the H_2-enriched M flame may feature significantly different response characteristics in comparison with the dihedral V flame.

In order to elucidate the underlying physics, twelve successive phase-resolved CH* chemiluminescence images

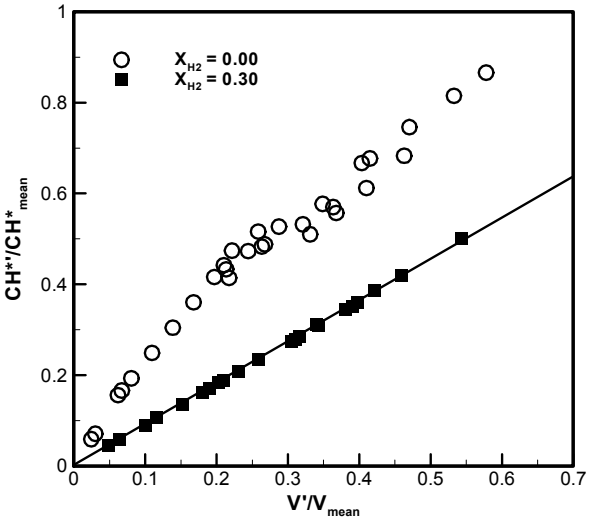

Figure 7. The normalized heat release response as a function of modulation amplitude at a modulation frequency of 200 Hz. Inlet conditions: T_{in} = 200 °C, V_{mean} = 60 m/s, ϕ = 0.60, and X_{H2} = 0.00, 0.30.

taken during a single cycle at a modulation frequency of 200 Hz and amplitude of V'/V_{mean} = 25% are illustrated in Figure 8. Line-of-sight integrated, background corrected images at the phases 90, 150, 210, and 270° are also presented for comparison. The figure shows that with H_2-enrichment (X_{H2} = 0.30), the spatial distribution of the reaction zone becomes very compact in both axial and radial directions. It is obvious from Figure 8 (A) that the flame angle variation is substantial during a modulation cycle. In the case of V flames, however, the flame oscillates in the flow direction, which means that the overall flame length changes over a period of perturbations, as shown in Figures 3 and 4. This result demonstrates that the dynamics of M flames is significantly different from that of V flames. The flame angle and CH* chemiluminescence intensity variations over one period of oscillation are shown in Figure 9. It can be seen that the variations in flame angle and CH* chemiluminescence intensity are out of phase. As the flame moves back (largest flame angle, see the phase 180°), the flame brush is almost vertical with respect to the flow direction and the CH* chemiluminescence intensity is low due to decreased flame area. These oscillations in the flame position (angle) result from fluctuations in the outer shear layer. It has been reported that if the shear layers in the swirl-stabilized gas turbine combustor are acoustically excited to form a coherent vortex ring structure, the inner shear layer rolls up inward and the outer shear layer rolls up outward [2, 32]. Note that even though periodic formation and convection of vortex structures occurs at φ = 210−270°, the flame response remains in the linear regime, as shown in Figure 7. The formation and convection of large scale structures are determined by fluid dynamic conditions, such as inlet velocity, forcing frequency, and amplitude. As already shown in Figures 2 (A) and 4, for a given set of fluid dynamic conditions the inverted V flame with long flame length exhibits strong interaction with a large scale structure, leading to highly nonlinear behavior. In contrast, an M flame is less influenced by the Kelvin-Helmholtz instability, since the relative ratio of convective time to the acoustic forcing period is very small, $\tau_{M-flame} < \tau_{V-flame}$. Furthermore, the M flame oscillates such that the flame angle varies significantly over a period of oscillation. The convection of a vortex structure is mainly determined by the mean flow, implying that the flame and the vortex structure exist in different paths for most of a given period. Hence there is not enough time for the coherent structure to interact with the flame. This further suggests that shedding of a large scale structure is not a sufficient condition for the nonlinear response of swirl-stabilized flames to acoustic excitation; the interaction between the structure and the flame plays a more important role.

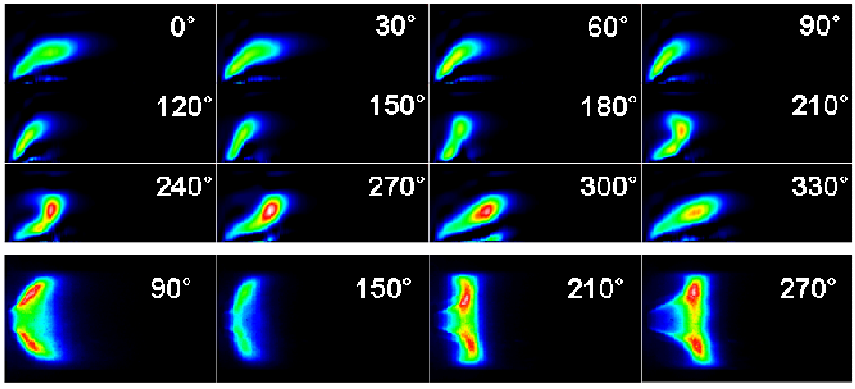

Figure 8. (A) Phase-synchronized deconvoluted CH* chemiluminescence images at a modulation frequency of f = 200 Hz and V'/V_{mean} = 25% (top), (B) line-of-sight integrated CH* chemiluminescence images at φ = 90°, 150°, 210°, and 270° (bottom). Inlet conditions: T_{in} = 200 °C, V_{mean} = 60 m/s, ϕ = 0.60, and X_{H2} = 0.30.

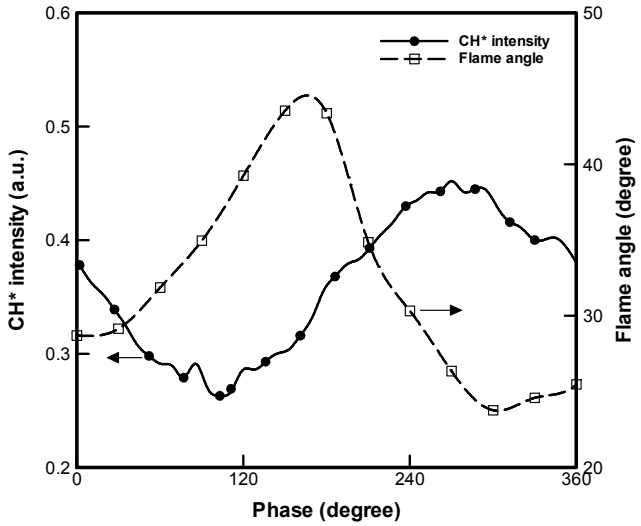

Figure 9. Time traces of global CH* chemiluminescence intensity and flame angle over one period of oscillation. Inlet conditions: T_{in} = 200 °C, V_{mean} = 60 m/s, ϕ = 0.60, and X_{H2} = 0.30, f = 200 Hz, and V'/V_{mean} = 25%.

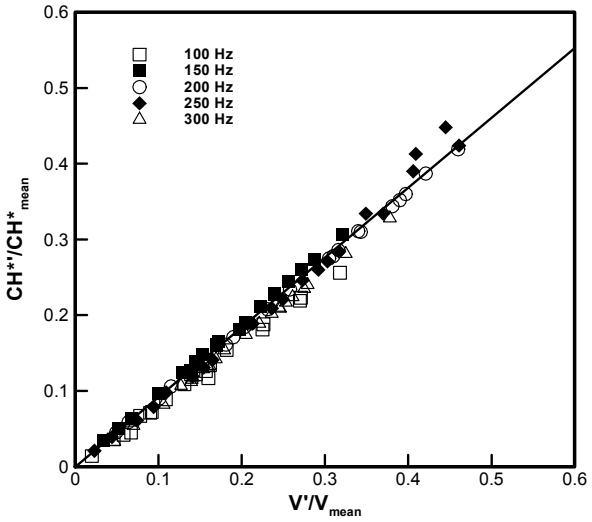

Figure 10. The normalized heat release response plotted as a function of forcing amplitude for a range of forcing frequency from 100 to 300 Hz. Inlet conditions: T_{in} = 200 °C, V_{mean} = 60 m/s, ϕ = 0.60, and X_{H2} = 0.30.

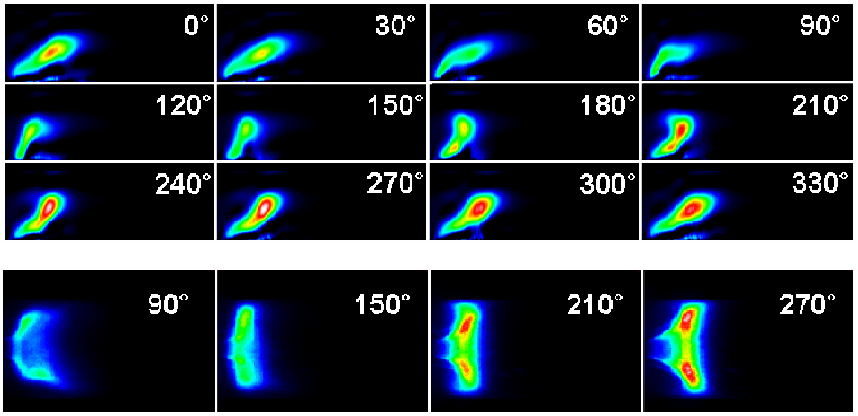

Figure 11. (A) Phase-synchronized deconvoluted CH* chemiluminescence imaging at a modulation frequency of f = 300 Hz and V'/V_{mean} = 30% (top). (B) Line-of-sight integrated, background-corrected CH* chemiluminescence images at φ = 90, 150, 210, and 270° (bottom). Inlet conditions: T_{in} = 200 °C, V_{mean} = 60 m/s, ϕ = 0.60, and X_{H2} = 0.30.

Figure 10 shows the normalized CH* chemiluminescence intensity plotted as a function of forcing amplitude for the range of frequency 100−350 Hz. Unlike the cases without H_2-enrichment at the same inlet flow condition, the flame tends to remain in the linear regime even at high forcing frequency (f = 300 Hz) and amplitude (V'/V_{mean} = 0.351). This result shows good agreement with data from a theoretical study by Lieuwen [33]. He reported that the response of the conical flame is nearly linear over the entire velocity disturbance amplitude, while the V flames exhibit substantial nonlinearity, which is manifested as saturation. This evidence strongly suggests that the flames with enveloped M configuration are more stable than inverted V flames in terms of combustion instability. The modification of the steady-state flame configuration from a V to an M geometry by H_2-enrichment was found to reduce the limit-cycle pressure oscillation amplitude significantly [34]. It is interesting to note that in contrast with V flames, the normalized heat release response of M flames is insensitive to the forcing

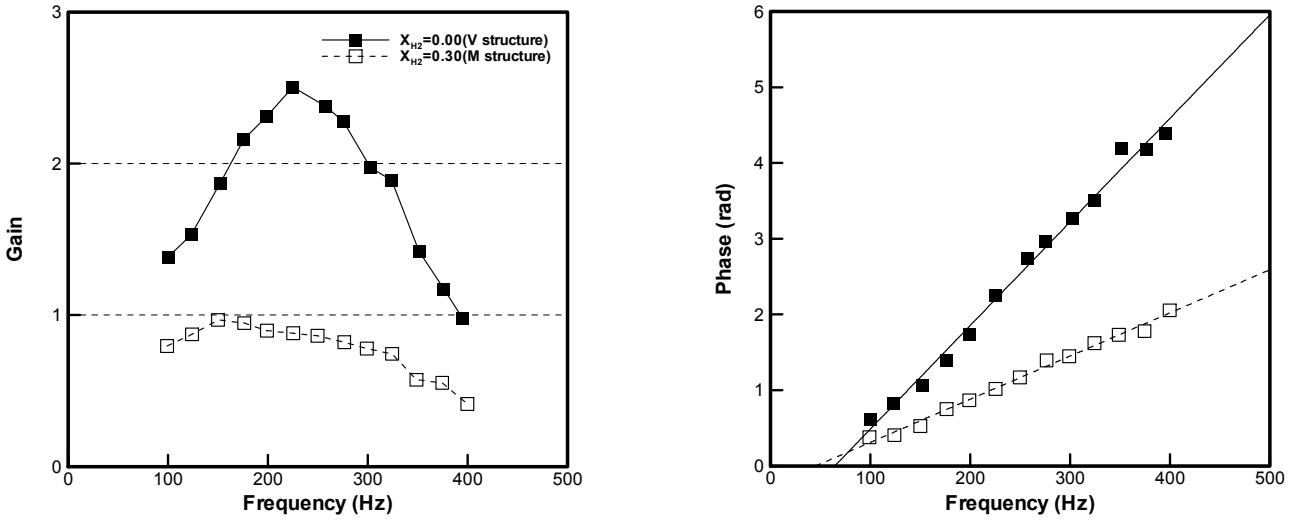

Figure 12. The gain and phase of the flame transfer function as a function of modulation frequency at a constant forcing amplitude, V'/V_{mean} = 0.100. Inlet conditions: T_{in} = 200 °C, V_{mean} = 60 m/s, ϕ = 0.60, and X_{H2} = 0.00, 0.30.

frequencies, as shown in Figure 10. The measured CH* chemiluminescence intensity for a range of frequencies 100−300 Hz overlaps on the same straight line. This can be attributed to the fact that the dynamics of the M flame is less influenced by the formation and convection of large-scale structures, which is by nature dependent on perturbation frequency. The normalized CH* chemiluminescence intensity starts to decrease when the modulation frequency is greater than 350 Hz (not shown).

Figure 11 shows phase-resolved CH* chemiluminescence images at a forcing frequency of 300 Hz and amplitude of 30% at the same inlet conditions as those shown in Figure 8. It can be concluded from Figures 8 and 11 that the dynamics of acoustically forced flames appear very similar, regardless of the forcing frequencies and amplitudes. The reason is that the response of the flames is linear in both cases and the forced response is independent of forcing frequencies. Under the conditions investigated here, shear layer rollup does not play an important role in inducing nonlinearity.

The flame transfer functions in frequency domain are presented in Figure 12. The velocity modulation amplitude was maintained at a constant value of V'/V_{mean} = 10%. At this condition, the forced flame response is linear below the level of acoustic velocity perturbation of V'/V_{mean} = 10%. As reported by recent studies [2, 27, 28], the global flame response can be described as a low-pass filter, in that the gain decreases as the frequency increases. These results also show that with increasing X_{H2}, the maximum gain of the flame transfer function decreases significantly and the phase decreases at a given forcing frequency, indicating that the gain depends strongly on flame length and steady-state flame configurations. For the inverted V flames, the gain of the flame transfer function exceeds unity at the modulation frequency of $100 \leq f \leq$ 375 Hz, indicating that the flame amplifies flow perturbation at certain frequencies. In the case of M flames, however, the overshoot behavior is not observed, i.e., the gain is less than unity, suggesting that M flames damp upstream flow perturbations. Also, the gain is almost independent of forcing frequency when the frequency is less than 300 Hz. At high forcing frequencies, the gain asymptotically approaches zero. The phase of V flames is greater than that of M flames, due to the fact that the convection time for velocity disturbances to reach the flame increases with increasing the flame length. The phase increases almost linearly with frequency, confirming that the influence of flow disturbances on the flame's heat release is purely convective.

In the present article, the combustion response of turbulent premixed flames to acoustic oscillations was experimentally determined. The effects of spatio-temporal fluctuations of equivalence ratio nonuniformities were not considered, however. In a real gas turbine engine environment, mixture ratio oscillations can be induced in the mixing section, since fuel is generally injected at the swirl vanes or near the inlet of the combustion chamber to avoid auto-ignition and improve mixing of the fuel and air mixture. In this situation, the flame responds to both perturbations of acoustic velocity and equivalence ratio. From a scientific point of view, an experimental investigation of the response of a partially premixed flame raises many challenging questions. First, the linear/nonlinear response of a partially premixed flame subjected to acoustic velocity and fuel/air ratio modulations is expected to be appreciably different, both quantitatively and qualitatively, as compared to

the response of a premixed flame. The combined effects of two inlet disturbances may induce partial extinction of the reaction zone at certain inlet flow conditions, particularly when the combustor is operated near lean blowoff limits. Also, a systematic parametric study on the response of a partially premixed flame should be performed to illustrate the role of inlet disturbances in controlling the flame's response characteristics and to elucidate the controlling physics. This work is left for future studies.

CONCLUSIONS

Nonlinear features of acoustically excited swirl-stabilized lean-premixed flames are characterized by nonlinear flame transfer function measurements and a phase-resolved analysis. Two distinct mechanisms of nonlinearity are investigated. The first mechanism is shear layer dynamics, which plays a key role in causing the nonlinearity of inverted dihedral V flames when the modulation amplitude is less than 40% at a modulation frequency of 200 Hz. H_2-enriched enveloped M flames are found to be more stable in terms of combustion instability. Their interaction with a large-scale coherent structure is negligible, which leads to a linear response even at high forcing frequency and amplitude. This implies that steady-state flame configuration is one of the important controlling parameters determining linear and nonlinear dynamics. The second mechanism of nonlinearity is unsteady flame liftoff which causes rapid reduction in the flame surface area due to a merging of two flame branches. This mechanism is manifested when the forcing amplitude is greater than 40%. A systematic investigation of forced flame response measurements with special emphasis on the effects of fuel composition variation will be useful to develop and validate theoretical tools to predict combustion instability phenomena in fuel-flexible gas turbine engines.

ACKNOWLEDGMENTS

Funding for this research was provided by the Department of Energy University Coal Research Program through Contract # DE-FG26-07NT43069 and the National Science Foundation through Award #0625970.

REFERENCES

[1] Lieuwen, T. and Yang, V., 2005, Combustion Instabilities in Gas Turbine Engines. Progress in Astronautics and Aeronautics, **210**, AIAA, Washington, DC.

[2] Balachandran, R., Ayoola, B.O., Kaminski, C.F., Dowling, A.P., and Mastorakos, E., 2005, Experimental investigation of the nonlinear response of turbulent premixed flames to imposed inlet velocity oscillations. Combust. Flame, **143**, 37−55.

[3] Bellows, B.D., Neumeier, Y., and Lieuwen, T., 2006, Forced response of a swirling, premixed flame to flow disturbances. J. Propul. Power, **22**, 1075−1084.

[4] Kulsheimer, C. and Buchner, H., 2002, Combustion dynamics of turbulent swirling flames. Combust. Flame, **131**, 70−84.

[5] Armitage, C.A., Balachandran, R., Mastorakos, E., Cant, R.S., 2006, Investigation of the nonlinear response of turbulent premixed flames to imposed inlet velocity oscillations. Combust. Flame, **146**, 419−436.

[6] You, D., Huang, Y., and Yang, Y., 2005, A generalized model of acoustic response of turbulent premixed flame and its application to gas-turbine combustion instability analysis. Combust. Sci. Tech., **177**, 1109−1150.

[7] Preetham, S.H. and Lieuwen, T., 2007, Response of turbulent premixed flames to harmonic acoustic forcing. Proc. Combust. Inst., **31**, 1427−1434.

[8] Fleifil, M., Annaswamy, A.M., Ghoneim, Z.A., and Ghoniem, A.F., 1996, Response of a laminar premixed flame to flow oscillations: a kinematic model and thermoacoustic instability results. Combust. Flame, **106**, 487−510.

[9] Roux, A., Gicquel, L.Y.M., Sommerer, Y., and Poinsot, T.J., 2008, Large eddy simulation of mean and oscillating flow in a side-dump ramjet combustor. Combust. Flame, **152**, 154−176.

[10] Sengissen, A.X., Van Kampen, J.F., Huls, R.A., Stoffels, G.G.M., Kok, J.B.W., and Poinsot, T.J., 2007, LES and experimental studies of cold and reacting flow in a swirled partially premixed burner with and without fuel modulation. Combust. Flame, **150**, 40−53.

[11] Staffelbach, G., Gicquel, L.Y.M., Boudier, G., and Poinsot, T., 2009, Large eddy simulation of self excited azimuthal modes in annular combustors. Proc. Combust. Inst., **32**, 2909−2916.

[12] Huang, Y. and Yang, V., 2009, Dynamics and stability of lean-premixed swirl-stabilized combustion. Prog. Energy Combust. Sci., **35**, 293−364.

[13] Kim, K.T., Lee, J.G., Quay, B.D., and Santavicca, D.A., 2010, Response of partially premixed flames to acoustic velocity and equivalence ratio perturbations. Combust. Flame, **157**, 1731−1744.

[14] Kim, K.T., Lee. J.G., Quay, B.D., and Santavicca, D.A., 2010, Spatially distributed flame transfer functions for predicting combustion dynamics in lean premixed gas turbine combustors. Combust. Flame, **157**, 1718−1730.

[15] Lieuwen, T., McDonell, V., Santavicca, D., and Sattelmayer, T., 2008, Burner development and operability issues associated with steady flowing syngas fired combustors. Combust. Sci. Technol., **180**, 1167−1190.

[16] Richards, G.A., McMillian, M.M., Gemmen, R.S., Rogers, W.A., and Cully, S.R., 2001, Issues for low-emission, fuel-flexible power systems. Prog. Energy Combust. Sci., **27**, 141−169.

[17] Strakey, P., Sidwell, T., and Ontko, J., 2007, Investigation of the effects of hydrogen addition on lean extinction in a swirl stabilized combustor. Proc. Combust. Instit. **31**, 3173−3180.

[18] Schefer, R.W., 2003, Hydrogen enrichment for improved

lean flame stability. Int. J. Hydrogen Energ., **28**, 1131−1141.
[19] Jackson, G.S., Sai, R., Plaia, J.M., Boggs, C.M., and Kiger, K.T., 2003, Influence of H_2 on the response of lean premixed CH_4 flames to high strained flows. Combust. Flame, **132**, 503−511.
[20] Cozzi, F. and Coghe, A., 2006, Behavior of hydrogen-enriched non-premixed swirled natural gas flames. Int. J. Hydrogen Energ., **31**, 669−677.
[21] Kido, H., Nakahara, M., Nakashima, K., and Hashimoto, J., 2002, Influence of local flame displacement velocity on turbulent burning velocity. Proc. Combust. Instit., **29**, 1855−1861.
[22] Sarli, V. and Benedetto, A., 2007, Laminar burning velocity of hydrogen-methane/air premixed flames. Int. J. Hydrogen Energ., **32**, 637−646.
[23] Mandilas, C., Ormsby, M.P., Sheppard, C.G.W., and Wooley, R., 2007, Effects of hydrogen addition on laminar and turbulent premixed methane and iso-octane-air flames. Proc. Combust. Instit., **31**, 1443−1450.
[24] Schefer, R.W., Wicksall, D.M., and Agrawal, A.K., 2002, Combustion of hydrogen-enriched methane in a lean premixed swirl-stabilized burner. Proc. Combust. Instit., **29**, 843−851.
[25] Wicksall, D.M., Agrawal, A.K., Schefer, R.W., and Keller, J.O., 2005, The interaction of flame and flow field in a lean premixed swirl-stabilized combustor operated on H_2/CH_4/air. Proc. Combust. Instit., **30**, 2875−2883.
[26] Wicksall, D.M. and Agrawal, A.K., 2007, Acoustics measurements in a lean premixed combustor operated on hydrogen/hydrocarbon fuel mixtures. Int. J. Hydrogen Energ., **32**, 1103−1112.
[27] Kim, K.T., Lee, J.G., Lee, H.J., Quay, B.D., and Santavicca, D.A., 2010, Characterization of forced flame response of swirl-stabilized turbulent lean-premixed flames in a gas turbine combustor. J. Eng. Gas Turb. Power, **132**, 04.
[28] Durox, D., Schuller, T., Noiray, N. and Candel, S., 2009, Experimental analysis of nonlinear flame transfer functions for different flame geometries. Proc. Combust. Inst., **32**, 1391−1398.
[29] Thumuluru, S.K. and Lieuwen, T., 2009, Characterization of acoustically forced swirl flame dynamics. Proc. Combust. Inst., **32**, 2893−2900.
[30] Schuller, T., Durox, D., and Candel, S., 2003, Self-induced combustion oscillations of laminar premixed flames stabilized on annular burners. Combust. Flame, **135**, 525−537.
[31] Schuller, T., Durox, D., and Candel, S., 2003, A unified model for the prediction of laminar flame transfer functions: comparisons between conical and V-flame dynamics. Combust. Flame, **134**, 21−34.
[32] Cala, C.E.C, Fernandes, E.C., and Heitor, M.V., 2002, Analysis of oscillating shear layer. 11th Symposium on Application of Laser Techniques and Fluid Mechanics, Lisbon, Portugal.
[33] Lieuwen, T., 2005, Nonlinear kinematic response of premixed flames to harmonic velocity disturbances. Proc. Combust. Inst., **30**, 1725−1732.
[34] Kim, K.T., Lee, H.J., Lee, J.G., Quay, B., and Santavicca, D., 2009, Flame transfer function measurement and instability frequency prediction using a thermoacoustic model. ASME paper GT2009−60026.